



Effects of WC grain size and Co content on microscale wear behavior of micro end mills in aluminum alloy 7075 machining

Peng Gao¹ · Xibin Wang^{1,2} · Zhiqiang Liang^{1,2} · Junfeng Xiang³ · Wei Li¹ · Jiaqing Xie¹

Received: 1 October 2018 / Accepted: 19 June 2019 / Published online: 5 July 2019
© Springer-Verlag London Ltd., part of Springer Nature 2019

Abstract

The effects of cemented carbide materials on cutting edge fracture mechanism of micro end mills in aluminum alloy 7075 machining are investigated. A series of micro milling experiments on the tool wear were conducted. The surface morphologies of micro end mills were observed, and the end teeth flank wear length and tool total cutting edge length reduction were measured. The results showed that the Co content and WC grain size of cemented carbides have significant effects on tool wear and cutting performance of the micro end mill. With increase of WC grain size, the tool end teeth flank wear length increases and the total cutting edge length reduction of the mill obviously increases. Thus, the micro end mill with finer grain size presents better wear resistance. However, with increase of Co content, the micro end mill exhibits less wear resistance. This can be explained that the adsorption energy between Co atom and Al atom become larger based on first principle calculation of adsorption energy between cemented carbides and aluminum alloy. The Co binder of tool material is dragged off by frequent fall off of built-up edge, resulting in more loss of Co element. Thus, the strength of the tool is decreased.

Keywords Tool wear · Micro end mill · Cemented carbides · Wear mechanism

1 Introduction

Aluminum alloys have been increasing on demand and widely applied in automotive, mold, and aeronautic industries due to the lighter products without losing quality [1]. As the typical Al-Zn-Mg-Cu series high-strength alloy, aluminum alloy 7075 has good chemical resistance, outstanding strength-to-density ratio, and relatively low densities, which is widely used in micro-fluidic devices, micro-scale heat sinks, micro-propellers, and so on [2]. Different types of cemented carbides have important effects on wear resistance and fracture resistance of cutting tools. Especially for micro tools, the tools are more prone to adhesive wear and tool edge fracture. In micro milling, the micro tools are easily worn at the early stage and the tool life is difficult to meet the requirements of micro products machining [3]. Appropriate material selection of micro end mill could improve its cutting performance and service life. The tool materials require high wear and fracture resistance and good cutting performance. Cemented carbides are widely applied in cutting tools due to their high hardness and wear resistance [4]. The WC grain size and cobalt content of cemented carbides have significant effects on cutting performance and tool life of micro end mill. Fracture toughness and fatigue crack growth resistance of cemented carbides

✉ Zhiqiang Liang
liangzhiqiang@bit.edu.cn

Peng Gao
gaoqindao@126.com

Xibin Wang
cutting0@bit.edu.cn

Junfeng Xiang
xiang_junfeng@126.com

Wei Li
lliw@bit.edu.cn

Jiaqing Xie
xiejq@nwafu.edu.cn

¹ School of Mechanical Engineering, Beijing Institute of Technology, Beijing 100081, People's Republic of China

² Key Laboratory of Fundamental Science for Advanced Machining, Beijing Institute of Technology, Beijing 100081, China

³ School of Electromechanical and Automotive Engineering, Yantai University, Yantai 264005, China

sensitively depend on Co content and WC grain size, while fatigue sensitivity depends significantly on carbide contiguity or binder thickness [5]. The reasonable tool material type selection is an effective way to improve tool life of cemented carbide micro end mill.

Some research works were carried out on the effects of Co content and WC grain size of cemented carbides on cutting performance and service life of cutting tools. Guo et al. [6] found that the ultrafine cemented carbide tools that possess better hardness and transverse rupture strength suffered from slight adhesive wear and abrasive wear in cutting AISI 1045 carbon steel. Similarly, the medium grain size presented serious adhesive and abrasive wear on flank face and rake face of tool. Kai et al. [7] reported the tool life of micro-tool fabricated using cemented carbides with 90 nm grain size was longer than that of the tool with 0.6 μm grain size, presumably because the former has better fracture resistance and forming accuracy. Jawaid et al. [8] reported the flank face wear rate of cemented carbide inserts with 0.68 μm grain size was greater than that with 1.0 μm grain size. Pirso et al. [9] found the wear resistance of cemented carbides depends on material hardness and chemical composition, and the wear rate decreases with the increase in hardness and decrease in binder content. Saito et al. [10] found that tool wear increases with increasing of WC grain size and Co content. Specifically, the wear rate is linearly proportional to the Co mean free path and wear resistance is proportional to hardness. Chen et al. [11] reported that the WC-5TiC-0.5VC-8Co cemented carbide tool with finer grain size has longer tool life and its main wear mechanism is adhesion wear and oxidation when machining HT250 gray cast iron. However, less study has focused on the effects of WC grain size and the Co content on microscale wear mechanisms of micro end mill. Additionally, the effects of different types of cemented carbides on the fracture damage mechanism and cutting performance of micro end mills remain unclear.

Several researchers have reported the investigation of the wear behavior of micro end mills. Li et al. [3] found the micro mill wear mainly presents abrasive wear and chipping due to the poor stiffness and strength of cutting edge. Kadirgama et al. [12] found that flank wear, chipping, cracking and catastrophic, plastic lowering at cutting edge are the dominant tool failure modes. Oliaei et al. [13] found tool wear of micro milling presents the increase of cutting edge rounding, flank wear, and reduction of tool diameter. List et al. [14] found the formation of built-up edge and adhesive layer on cemented carbide cutter rake face degrades the tool shape and efficiency in aluminum-copper alloy machining, and tool wear is caused by the activation of the diffusional and chemical phenomenon. Wang and Kwon [15] reported the wear modes of tool are adhesion and abrasion wear during the machining of pure aluminum, and the WC grains are pulled out due to the weakening of Co binder and the WC grains are also dislodged from

the tool surface. Chen et al. [16] reported that the tool wear mechanism of cemented carbide micro end mill presents abrasive wear, adhesive wear, diffusion wear, and oxidative wear. Konyashin and Ries [17, 18] reported that the near-nano cemented carbide tool wear mechanism presents micro-cracking and micro-chipping resulting in the detachment of large WC/Co agglomerates, and the medium grades are wearing binder leading to unsupported WC grain, WC grain micro chipping, detachment of WC grain, and WC-Co fragments. Although some research works were carried out on tool wear mechanism of micro milling, the tool wear mechanism of ultra-fine cemented carbide micro end mill is still unclear.

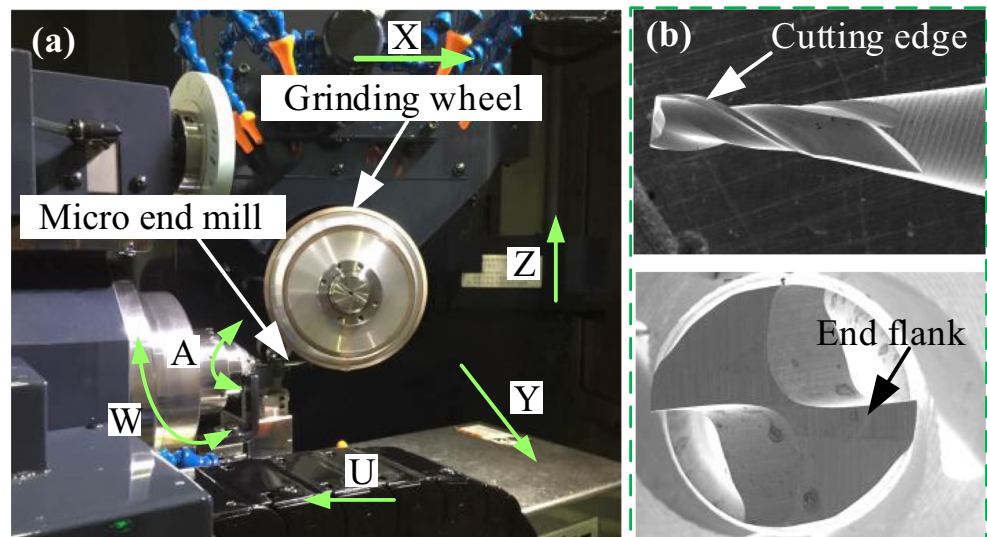
This study examines the effects of WC grain size and Co content on the microscale wear behavior of micro end mill in aluminum alloy 7075 machining. The tool wear experiments were carried out using various micro end mills fabricated with different type of cemented carbides. During the experiments, the surface wear morphologies of micro end mills were observed by scanning electron microscopy (SEM). The tool fracture mechanism of the cemented carbide micro end mills will be also discussed.

2 Fabrication of micro end mills

The four kinds of micro end mills with different tool materials K55SF, DK500UF, DK450UF, and DK120UF (GUHRING Co., Ltd.) are fabricated by using a six-axis CNC tool grinding machine (CNS7d, Makino Seiki Co., Ltd.) as shown in Fig. 1, which have the identical geometric parameters: diameter 0.5 mm, helix angle 30° , rake angle 3° , and relief angle 12° , as shown in Fig. 1(b). The position precision of the grinding machine in X-axis, Y-axis, and Z-axis is 3.5 μm , and repositioning precision the grinding machine in X-axis, Y-axis, and Z-axis is 1.5 μm . The resolution of the machine in X-axis, Y-axis, and Z-axis is 0.1 μm . The composition and mechanical properties of different cemented carbides are shown in Table 1. The fabricated micro end mills are cleaned using an ultrasonic cleaning machine. The tool surface morphology is observed by scanning electron microscopy (SEM, FEI Quanta 650FEG).

The surface morphologies of micro end mills end flank face with different types of cemented carbides are observed as shown in Fig. 2. The cutting edges of micro end mills with different types of cemented carbides present various characteristics of micro fracture and micro cracks. The micro end mill with finer WC grain size (K55SF) presents a better morphology, sharper cutting edges, less micro cracks, and shallower scratched micro grooves, compared with the tools with other three types of cemented carbides (Fig. 2), while the micro end mills with DK450UF appear brittle fracture due to larger grain size and higher WC content. The surface of micro end

Fig. 1 Fabrication of micro end mill. (a) Fabrication experimental setup. (b) Micro end mill



mill with DK500UF has more micro pits between phase boundaries. The larger WC particles will increase the surface damage, which leads to randomly distributed micro pits. The Co binders are extruded and removed from the phase boundaries of WC and Co leading to the generation of micro cracks or micro pits on the surface of micro end mill. The micro end mill with DK120UF also has sharper cutting edges and less grinding defects.

3 Tool wear experiments

The dry slot machining experiments using the fabricated micro end mill were conducted in a five-axis machining center DMU80 monoBLOCK (DMG MORI Co., Ltd.) as shown in Fig. 3. The resolution of the machining center in *X*-axis, *Y*-axis, and *Z*-axis is 1 μm , and the feed accuracy in *X*-axis, *Y*-axis, and *Z*-axis is 1 μm . Aluminum alloy 7075 was adopted as workpiece material. Initially, a clean-up cut on the workpiece surface was performed with a flat end mill with a diameter 10 mm to ensure the same depth of cut during the micro milling. During micro milling, the cutting speed was 20 m/min, the feed rate was 2

$\mu\text{m}/\text{z}$, and the depth of cut was 50 μm . The experiments were repeated three times. The micro tools and machined workpiece were cleaned with alcohol in ultrasonic cleaning machine before measurement. The surface morphologies of micro end mills were observed by scanning electron microscopy and 3D laser scanning microscope VK-X100 (Keyence Co., Ltd.).

4 Results and discussion

4.1 Wear morphology

Figure 4 shows surface wear morphologies of micro end mill end flank faces after machining for the cutting length of 480 mm. The micro end mill with finer WC grain size (K55SF) presents less wear width on the end flank face, and no obvious damage occurs at the cutting edge compared with that of DK500UF. Besides, for the micro end mill with DK120UF, slight damage occurs at the cutting edge. However, both micro end mills with DK500UF and DK450UF suffer from serious cutting edge fracture under the same cutting length. Moreover, the built-up edge (BUE) and built-up layer (BUL) occurs in micro end mill surface. The micro end mill (DK500UF) with higher Co content shows less wear resistance compared with that of DK450UF and DK120UF. It can be found that the Co content and WC grain size of cemented carbides have significant effects on the wear and fracture resistance of micro end mill.

Figure 5 shows wear morphologies of micro end mills with different types of cemented carbides after machining for a longer length. The micro end mill end faces are strongly adhered by the workpiece material aluminum alloy. The serious flank face wear in the cutting edge and

Table 1 Composition and mechanical properties of different cemented carbides

Property	K55SF	DK500UF	DK450UF	DK120UF
WC content (%)	91	88	91	93
Co content (%)	9	12	9	7
Grain sizes (μm)	0.2-0.5	0.5	0.5	0.5
Density (g/cm^3)	14.40	14.15	14.45	14.70
Hardness (HV_{30})	1920	1660	1870	1850
Category	/	K40/50	/	K05

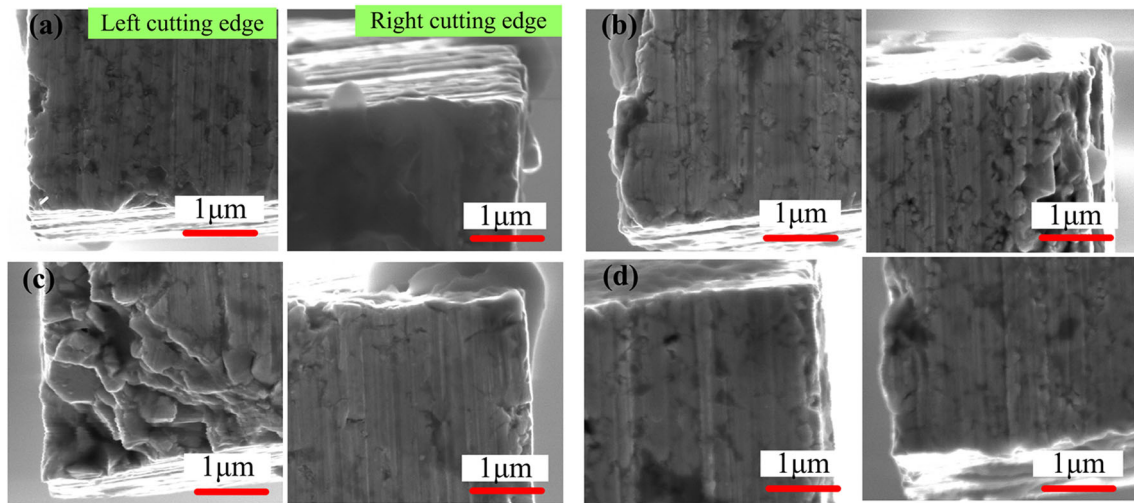


Fig. 2 Surface morphologies of micro end mill end flank faces fabricated with various types of cemented carbides. (a) K55SF, (b) DK500UF, (c) DK450UF, (d) DK120UF

the tool nose breakage result in the failure of micro mill. The micro end mill with finer cemented carbides (K55SF) possesses better fracture resistance, and after machining for 1200 mm, it still has a finer cutting edge and suffers from less wear. However, severe tool wear takes place on the micro end mill (DK500UF) even at the early cutting length of 520 mm and the tool material presents lower fracture resistance. Similarly, severe tool fractures are generated for the micro end mill (DK450UF), and even severe cutting edge damage occurs at the early cutting length of 560 mm, and this tool material also presents less fracture resistance. In contrast, the micro end mill (DK120UF) suffers from severe edge chipping at the cutting length of 720 mm (Fig. 5(d)). During micro milling, the aluminum alloy materials tend to be bonded to the cutting edge and this causes the formation of built-up edge under certain cutting speed conditions [14]. Moreover, the unstable built-up edge periodically breaks off, together with the scrape of a small lump of tool materials [19]. This also contributes to the formation of micro fracture on the cutting edge.

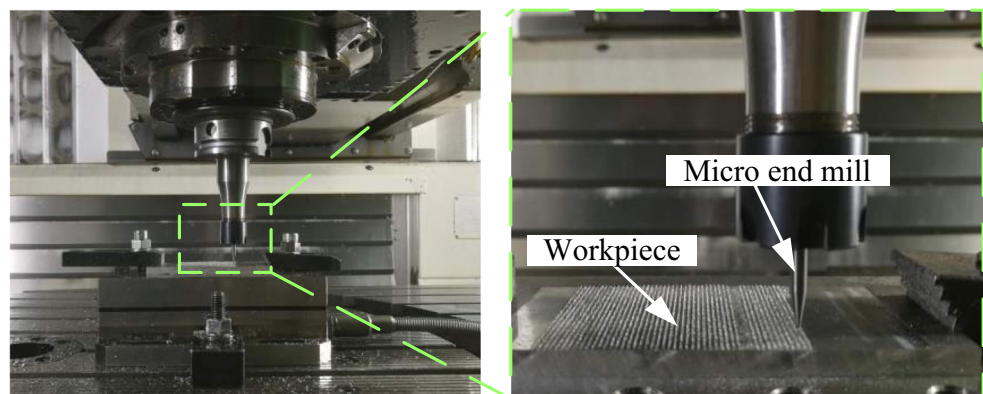
4.2 Edge chipping and crack morphologies of micro end mill

The edge chipping and crack morphologies of micro end mill (DK120UF) are shown as Fig. 6. The crack deflection is also observed from the crack morphologies. During micro milling, the cutting edge suffers from cyclic impact forces. The edge chipping of micro end mill mostly occurs at the tool nose where exists sharper cutting edge. Compared with macro milling, the cutting edge is easily broken due to weak strength. In the case of cemented carbides, the main toughening mechanism is ductile ligament reinforcement and the crack deflection is an additional toughening mechanism as the microstructure becomes coarser [20].

4.3 End teeth flank wear length and total cutting edge length reduction

To evaluate the effects of different types material on the tool wear of micro end mill, the end teeth flank wear length and the total cutting edge length reduction of micro end mill are

Fig. 3 Micro end milling experiment setup



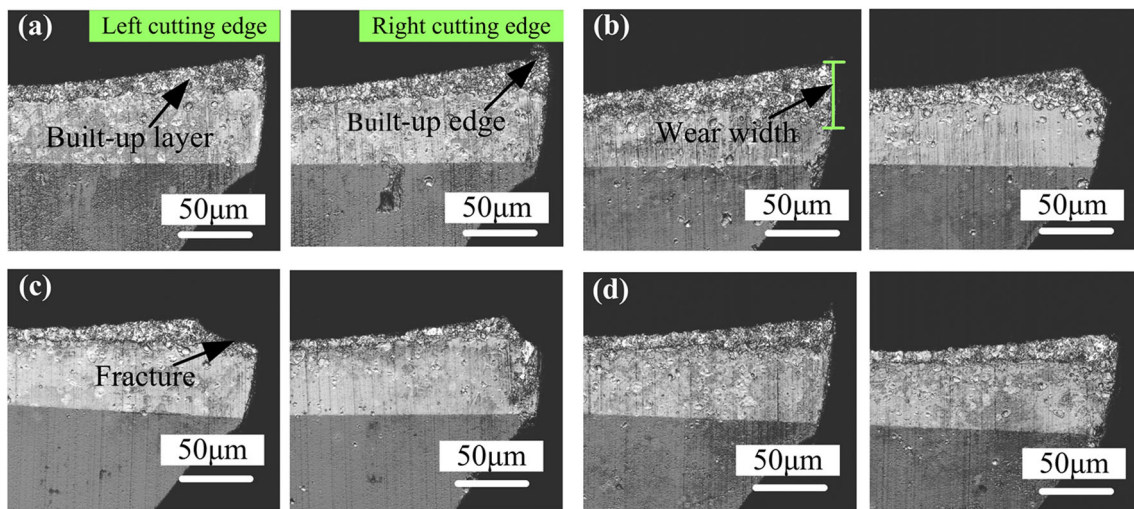


Fig. 4 Wear morphologies of micro end mill end flank faces after machining for the cutting length of 480 mm. (a) K55SF, (b) DK500UF, (c) DK450UF, (d) DK120UF

considered. The integrity of the tool edge was measured before experiments as shown in Fig. 7. The cutting edge length reduction is the original cutting edge length subtracting the total cutting edge length after wear. The measuring methods of micro end mill end teeth flank wear length and total cutting edge length reduction are shown in Fig. 7. The end teeth flank wear length of micro end mill increases rapidly when the tool early contacts with the workpiece materials. It can be seen that the tool wear width increases rapidly with the increase of cutting length in the case of the mill with DK500UF (Fig. 8(a)). The micro end mill fabricated using finer WC grain sizes 0.2–0.5 μm (K55SF) has a narrower tool wear width and a longer cutting length compared with the other three types of cemented carbide tools. However, the micro end mills with tool materials DK500UF, DK120UF, and DK450UF have a large tool end teeth flank wear length at the beginning of cutting length. Figure 8(b) shows the relationship of the total cutting edge length reduction of the mills with cutting length. It can be seen that, with increasing WC grain size, the total cutting edge length reduction of the mill obviously increases in the cases of the mills with tool material K55SF and DK450UF. The micro end mill with higher cobalt content generates early fractures on the cutting edge. The micro end mill with DK450UF has shorter tool life, and the micro tool exhibits tool breakage at a short cutting length of 240 mm. The micro end mill with material DK120UF also suffers from serious early broken. The micro end mills with finer WC grain size material can extend the micro end mill tool life.

4.4 Effects of WC/Co composition on the tool wear

The wear resistance of micro end mill is associated with the hardness of tool material. The hardness of the material

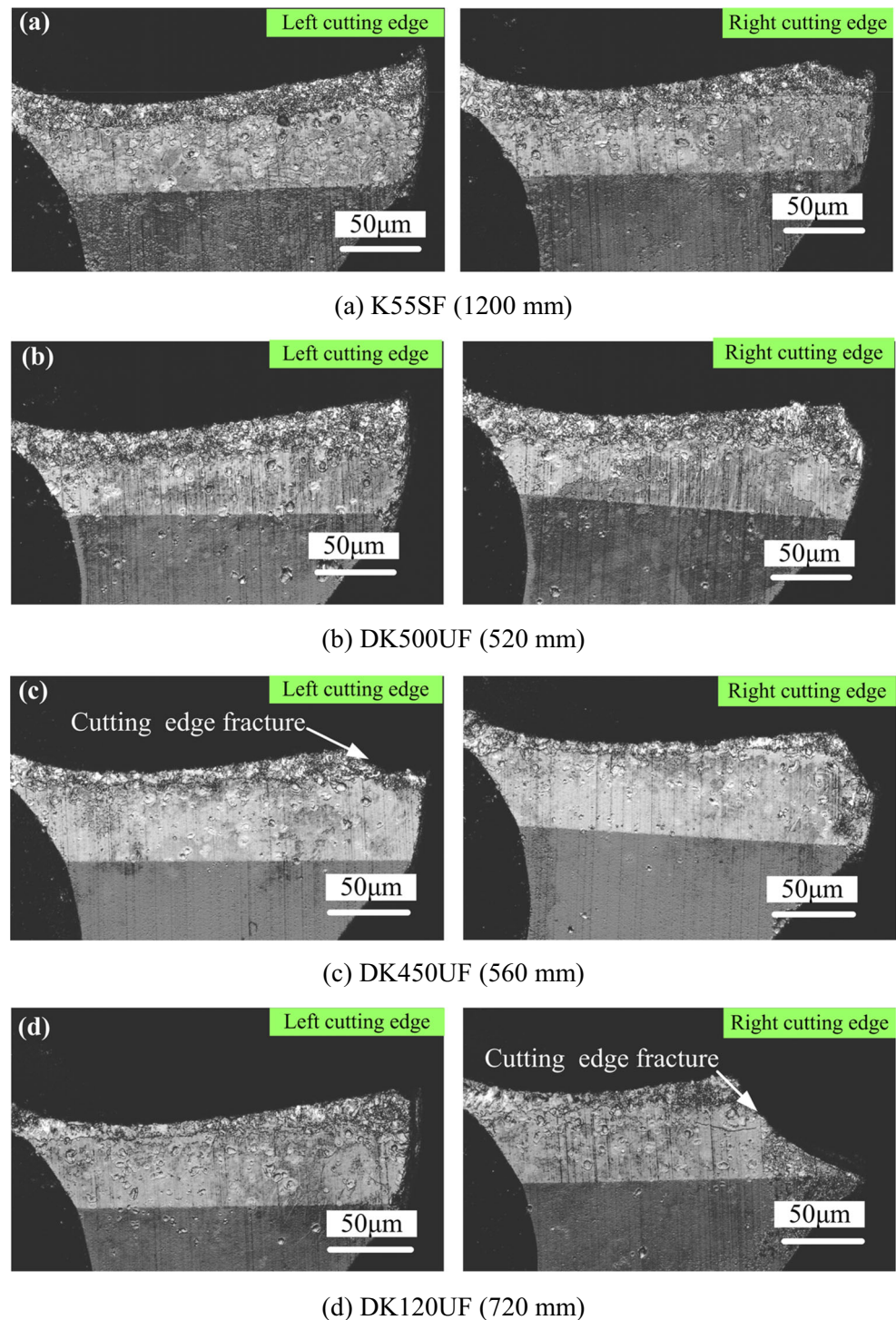
DK500UF is the least (1660 HV_{30}), and the tool end teeth flank wear length of the micro end mill is larger than that of others. Due to smaller WC grain size, the K55SF cemented carbides present higher hardness (1920 HV_{30}) leading to higher tool wear resistance. The wear rate reduces with decreasing both Co content and WC grain size of cemented carbides [10]. The mean free path in Co is closely related to plastic deformation ability of materials and greatly affects the material wear resistance. The mean free path can be evaluated as [21]:

$$\lambda_{Co} = \frac{\alpha d_{WC} V_{Co}}{1 - V_{Co}} \quad (1)$$

where d_{WC} is the WC grain size, V_{Co} is the Co content, and α is a factor which depends on the shape and contiguity of the carbide grains. The tool wear is related to the ratio λ_{Co}/α , and tool wear volume increases with the increase of the ratio [21]. The WC grain size and content of tool material decides the ratio λ_{Co}/α . The tool materials K55SF, DK500UF, DK450UF, and DK120UF ratio λ_{Co}/α can be obtained 0.0198, 0.0682, 0.0495, and 0.0376 as the expression (1), respectively. It can be seen that the tool end teeth flank wear length increases with the increase of the ratio (Fig. 8(a)). Therefore, in material selection of micro end mill the tool wear resistance can be evaluated by the ratio λ_{Co}/α .

In micro milling, with the increase of cutting length, the cutting edge radius becomes larger and micro chipping occurs in the cutting edge. Under high pressure, the workpiece materials tend to be adhered on the surface of micro end mill in the contact zone and the workpiece materials are welding to tool surface forming an adhesion layer. The tool wear is mainly caused by the formation of a built-up edge and an adhesion layer [22]. Under dry conditions, the wear of cemented carbide tool is mainly caused

Fig. 5 Wear morphologies of micro end mills with different types of cemented carbides after machining for a longer length. (a) K55SF (1200 mm), (b) DK500UF (520 mm), (c) DK450UF (560 mm), (d) DK120UF (720 mm)



by the removal of Co binder followed by the fracture of intergranular boundaries and fragmentation of carbide grains [9]. Due to the mechanical adhesion mechanism, the primary built-up layer is formed quickly resulting in the cutting edge geometry and changed microstructure [23].

The tool cutting edges suffered cyclic flexural and compression stress during micro milling. Dislocation behavior occurs in WC/Co grain boundaries, and the micro cracks began

nucleation. Under the action of alternating stress, the initiation micro cracks begin to form, and then the micro cracks propagate resulting in cutting edge fracture. Besides, some WC grains in cutting edge generated micro cracks under high-stress impact. When the micro cracks in the micro end mill cutting edge propagate, the WC grains of cutting edge are loosened and then pulled out [24]. Due to the viscous property of aluminum alloy, there is a strong bond between the tool

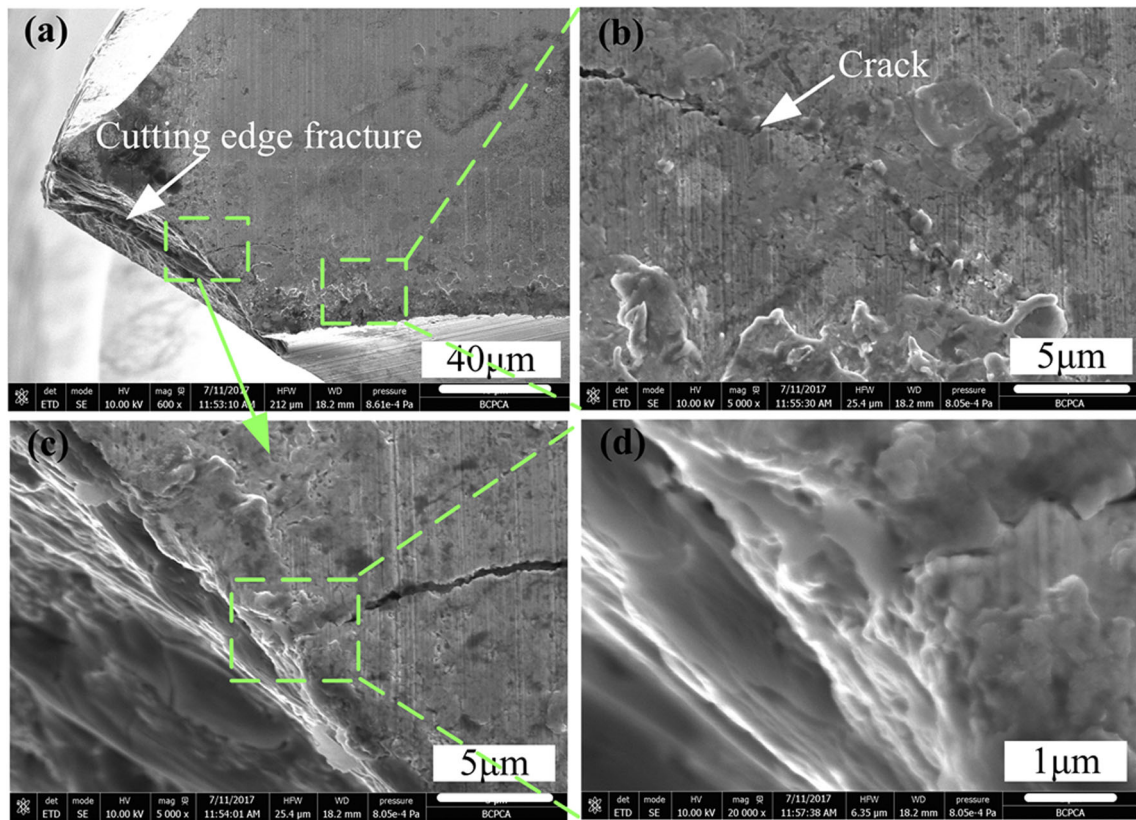


Fig. 6 Edge chipping and crack morphologies of micro end mill (DK120UF)

surface and workpiece. Some WC grains are pulled out leaving micro fracture in the cutting edge. The finer WC grain is not prone to produce dislocation for the small strain with a short slip surface. The finer grain size tool material K55SF has stronger fracture resistance compared with DK450UF. The cutting edge tool wear of micro end mill is related to the mean free path in Co, and the mean free path in Co λ_{Co} can be estimated from [25]:

$$\lambda_{Co} = \frac{d_{WC} V_{Co}}{(1 - C_{WC})(1 - V_{Co})} \tag{2}$$

where C_{WC} is the contiguity of WC. The contiguity of WC C_{WC} can be estimated from [23]:

$$C_{WC} = 1.03 \exp(-5V_{Co}) \tag{3}$$

The tensile strength and compressive strength of tool material are relative to the microstructure of the WC/Co. The tensile strength R_m and compressive strength $R_{r,m}$ of cemented carbides can be estimated as [26]:

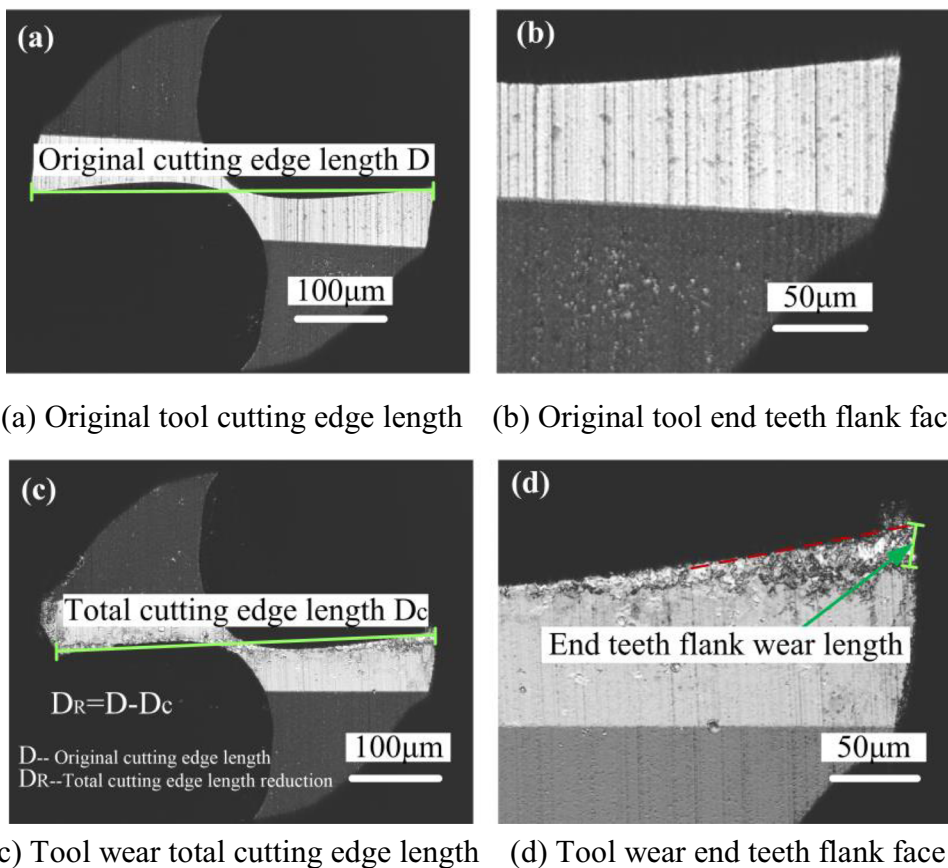
$$\sigma_m = \left[0.229 + 5.941V_{Co} - 4.536V_{Co}^2 + \frac{1}{\sqrt{d_{WC}}} (0.722 - 0.927V_{Co} + 3.673V_{Co}^2) \right] \sqrt{C} \tag{4}$$

$$\sigma_{rm} = \left[2.551 + 0.108V_{Co} - 1.238V_{Co}^2 + \frac{1}{\sqrt{d_{WC}}} (5.591 - 0.877V_{Co} - 3.046V_{Co}^2) \right] \sqrt{C} \tag{5}$$

The flexural strength σ_{bm} of brittle in bend test can be estimated as $\sigma_{bm} = 2\sigma_m$ [26]. The micro end mill with higher Co content (DK500UF) early appears with cutting edge tip fracture. The cemented carbides with higher Co content have higher static fatigue sensitivity and has less fatigue crack propagation resistance ability [27]. Due to the low flexural strength and hardness, the micro end mill with higher Co content tool materials (Table 2) early generates cutting edge fracture. Under cyclic stress, impact fatigue is a deterioration damage of cemented carbides and the actual stress is often lower than the material yield stress [28]. The oxidation also induces embrittlement of the Co binder phase along subcritical cracks, and the cemented carbide materials become more brittle and cracks propagate through the Co binder [28, 29].

The micro end mill with finer WC grain size (K55SF) generates tool broken at high cyclic times, and the tool presents higher fracture resistance. The fatigue fracture of larger WC grain size is dominated by WC grain bonding and fracture, and the finer WC grain size exhibits fatigue fracture [30]. The WC grain size and Co binder content of cemented

Fig. 7 Measurement of micro end mill cutting edge length and end flank face. (a) Original tool cutting edge length. (b) Original tool end teeth flank face. (c) Tool wear total cutting edge length. (d) Tool wear end teeth flank face



carbides have significant effects on the tool fracture mechanism. The cemented carbides exist critical Co free path M_c and critical WC grain size R_c , and the M_c and R_c reduce with increase of Co binder content [31]. When the mean free path in Co binder is lower than the critical the mean free path in Co binder M_c or the WC grain size is lower than the critical WC grain size R_c , intergranular fracture will become dominate in

fracture [31]. In the case of transgranular fracture, the WC grain sizes are usually larger than 1.0 μm , while the intergranular fracture grain sizes are smaller than 1.0 μm [31]. The grain sizes of cemented carbides are less than 1.0 μm (Table 1). The fracture of the tool cutting edges is dominant intergranular fracture. The nucleation of micro cracks usually occurs in the highest stress surface where the material defects

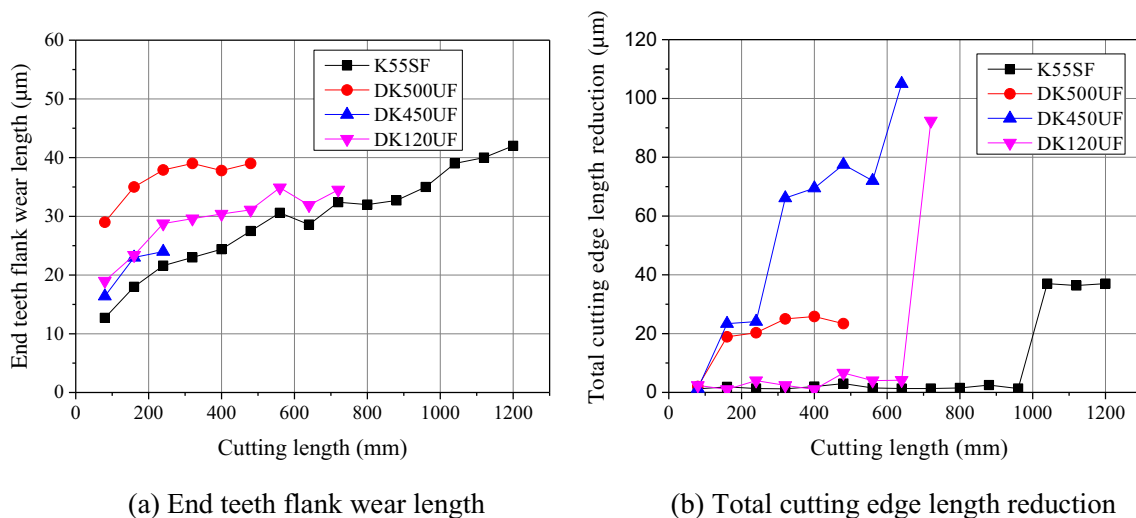


Fig. 8 End teeth flank wear length and the total cutting edge length reduction of micro end mills. (a) End teeth flank wear length. (b) Total cutting edge length reduction

Table 2 Mean free path in Co, contiguity of WC, tensile strength, compressive strength, and flexural strength of various grades of cemented carbides

Grade	λ_{Co}	C_{WC}	σ_m (GPa)	σ_{rm} (GPa)	σ_{bm} (GPa)
K55SF	0.058–0.144	0.66	1.36–1.81	8.38–12.04	2.76–3.62
DK500UF	0.157	0.57	1.37	7.73	2.74
DK450UF	0.144	0.66	1.36	8.38	2.72
DK120UF	0.137	0.73	1.35	8.84	2.7

exist. The defects conclude the flaw sizes are several times bigger than the mean WC grain size, plasticity confined to a zone process near-tip, and process zone governing fracture extends over a short distance [32, 33]. The fatigue fracture mainly originates from inhomogeneities such as aggregates of WC grains or micro pores [34].

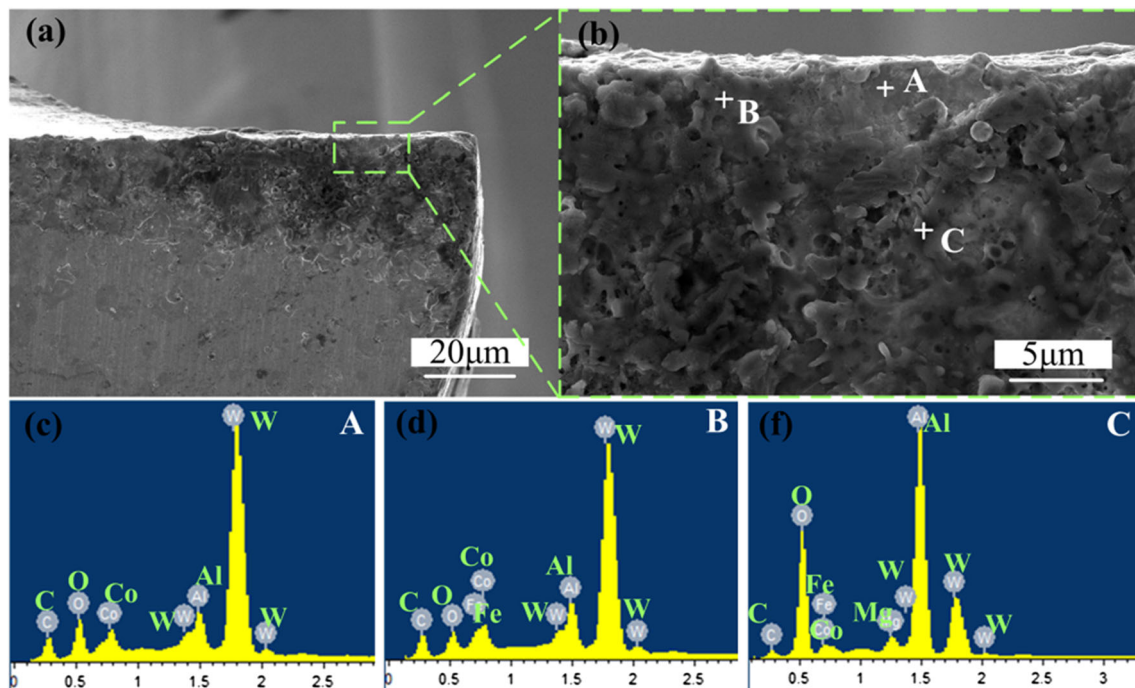
4.5 Adhesion wear mechanism of micro end mills

The surface wear morphology and EDS of micro end mill (K55SF) end teeth flank face at the cutting length of 1200 mm are shown in Fig. 9. It can be seen that the end teeth flank face is covered by BUL, and the element of dot A (Fig. 9(c)) is mainly Al. It indicates that the end teeth flank of the tool is mainly covered with the adhesive material aluminum alloy. Besides, the element of dot B and C is also mainly element Al and indicates that the end teeth flank of tool is covered with aluminum alloy. The friction surface WC grain of the tool is removed by shearing and stretching resulting in

adhesive wear due to relative movement between the tool and workpiece. Under high stresses, the WC grains in cutting edge are cracked and some WC grains are pulled out leaving micro fracture in the cutting edge. Due to the strong chemical affinity of aluminum alloy, the surface contact mode between the tool flank and workpiece material aluminum alloy is bonded contact.

The surface morphology and EDS of micro mill flank face (K55SF) at the cutting length of 1200 mm are shown in Fig. 10. The element of dot A is mainly the element Al indicating that the flank is covered with the adhesive workpiece materials. The BUL is found from the flank face of micro end mill, and the element Al appears in the falling off region as shown from dot B (Fig. 10B). The composition of built-up layer is similar to the aluminum alloy 7075. This proves that the element Al adheres on the tool surface. Due to the strong bond between tool and workpiece, the contact friction behavior between flank face and workpiece occurs resulting in serious adhesive wear. Due to the thermo-mechanical mechanisms, the aluminum alloy suffers from a process of incipient fusion of the metallic matrix and then, the visco-plastic state of aluminum welds onto the tool surface under cutting compression stress. Besides, once the BUL has been formed, initial cutting conditions change enabling BUE formation by mechanical adhesion [35]. The aluminum accumulated on tool surface will increase the thermal conductivity and reduce its initial hardness.

During micro milling, the end teeth flank face of micro end mill contacts the bottom of micro channel, and the end teeth flank face almost does not suffer from cutting force. However,

**Fig. 9** EDS of the adhesive wear end teeth flank surface (K55SF)

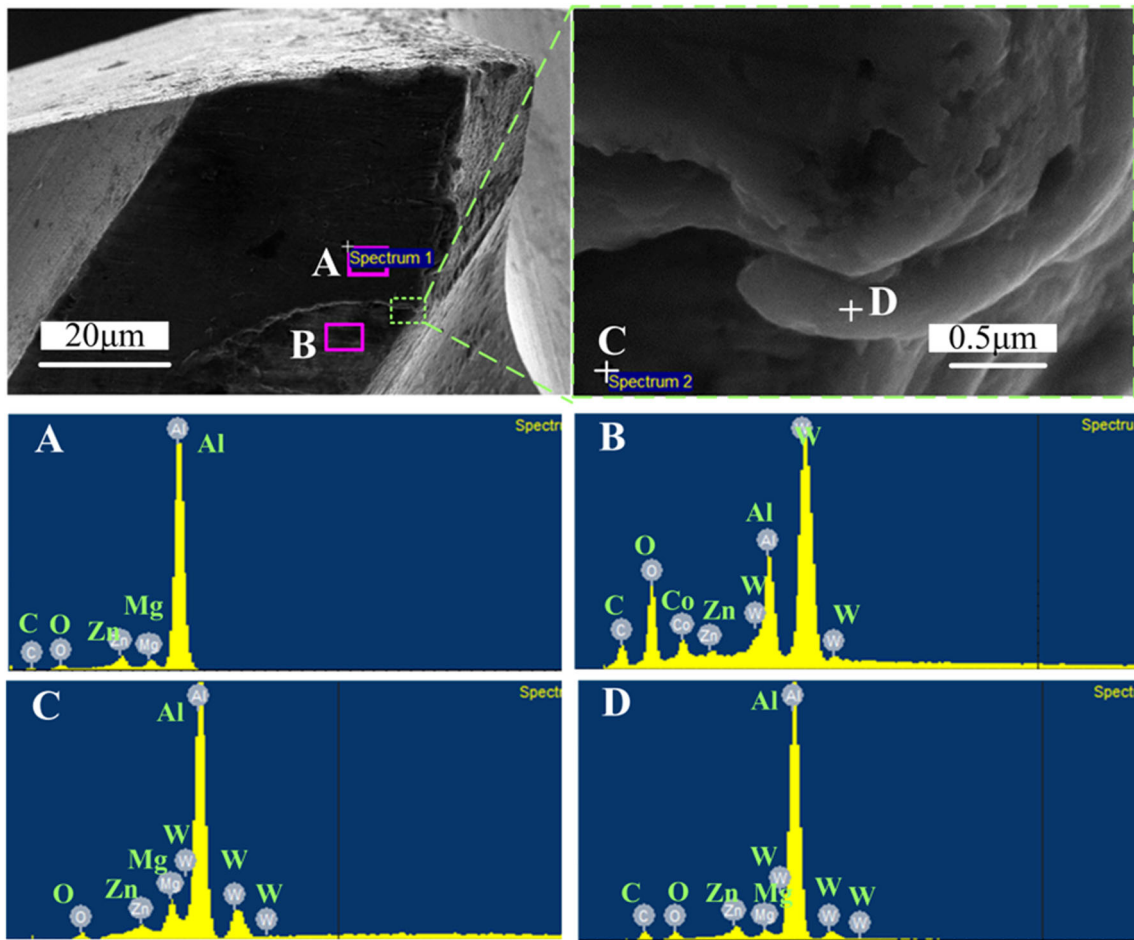


Fig. 10 Flank surface morphology and EDS of micro end mill (K55SF)

severe adhesive wear occurs on the end teeth flank faces. The reason is that the contact of micro milling is in meso-scale and adsorption energy becomes the key factors to dominate the flank face adhesion in microscale. The contact region of micro cutting tool in microscale is considered two rigid ball contacts. When the two surfaces contact, the adhesive force F_0 can be obtained as [36]:

$$F_o = 2\pi R_o \Delta\gamma \tag{6}$$

According to Derjaguin the two ball at a distance of h_0 , the adhesive force $F(h_0)$ be obtained:

$$F(h_o) = \frac{8\pi\Delta\gamma}{3} R_o \left[\left(\frac{\varepsilon}{h}\right)^2 - \frac{1}{4} \left(\frac{\varepsilon}{h}\right)^8 \right] \tag{7}$$

where R_o is the equivalent radius, h is the distance between molecules, ε is the equilibrium distance between molecules, the Dupre adhesive work $\Delta\gamma = A_o/16\pi\varepsilon^2$, and A_o is the Hamaker constant. It can be seen that, even the end teeth flank suffered no axial cutting force in theory, the end teeth flank of the tool also occurs serious adhesive wear under the adhesive force.

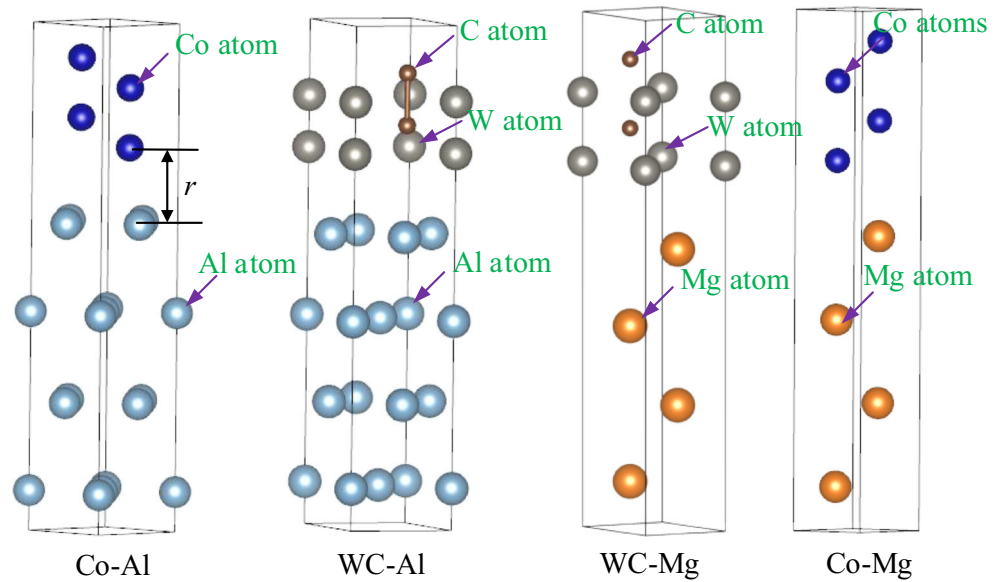
To further analyze the adhesion mechanism of micro milling in aluminum alloy 7075 machining, the first principle density functional theory (DFT) is used to calculate the adhesion process between the tool material and aluminum alloy 7075. Figure 11 shows the first principle calculation model of adsorption energy between micro end mill and aluminum alloy 7075. The PWMAT software is used to calculate the adsorption process, and the main elements of the aluminum alloy are considered. The formula for calculating adsorption energy by the first principle is as follows:

$$E_{\text{bind}} = E_{\text{complex}} - (E_A + E_B) \tag{8}$$

where E_{bind} is the binding energy, E_{complex} is the total energy of the system after adsorption, and E_A is the energy of the adsorbed material and the energy of E_B adsorption material.

First principle calculation of the adsorption energy between cemented carbides and aluminum alloy 7075 is shown in Table 3. It can be seen that the adsorption energy between Co atom in cemented carbides and Al atom in aluminum alloy is -7.2455 eV, so the adsorption force between the Co atom and the Al atom is larger. The WC grain and Co atom in

Fig. 11 First principle calculation model of interface bonding way between cemented carbides and aluminum alloy



cemented carbide will not adsorb the Mg atom in workpiece material. Besides, the WC grain also will not adsorb the Al atom. During the wear process of micro end mill, the adsorption energy between Co atom and Al atom is larger and the Co binder in the tool will be dragged off by frequent fall off of built-up edge, resulting in more loss of Co element, which makes strength of the tool lower. Moreover, under cutting pressure action, the Al_xCo_y intermetallic compounds are generated and can favor micro welding between the built-up layer and tool surface [14].

The adhesive wear damage mechanism of micro end mill is shown in Fig. 12. The WC grains are pulled out and dragged by the adjacent aluminum alloy, and the WC grains' dislocation, plastically deformed and broken, occur on the cutting contact. At early cutting stage, micro crack and WC particle loosening occurs in cutting edge. Due to removal of Co binder from the top layer of the WC grains, the WC grains become more prone to breaking out [23]. The adhesion of the aluminum alloy materials leads to the formation of built-up edge which tends to promote tool chipping, and unstable built-up edge periodically breaks off taking with a small lump of cutting edge [19]. The coarse grades demonstrated inhomogeneous behavior with pulling out of WC grains in cutting edge, followed by binder removal and scratching of WC at longer sliding distances, while the ultrafine grades showed homogeneous plowing behavior [13]. Under high pressure, tensile stresses are induced in the WC grain boundaries parallel to

cutting force, creating a driving force for Co binder diffusion into the grain boundaries. Besides, the WC grains are partly broken up by Co grain boundary infiltration and make GBS possible [37]. Under cutting force, the tool material deformation starts with dislocation movements in the Co binder and moves over to a gradual increase in GBS, accommodated by Co diffusion and dislocation climb in combination with dislocation movements and slip in the WC grains [37]. Under shearing stress, deformation and dislocations occur in WC grain and Co binder of tool surface resulting in large strains in the lattice. Besides, plastic deformation of tool materials also occur by grain boundary sliding, accommodated by Co binder infiltration of general grain boundaries and plastic deformation of WC grains [38]. The two materials contact and move, and the contact bond is sheered forming new contact bond.

Compared with the traditional milling, the size effect of micro milling is prevailing and the adhesive contact size effect also occurs. During micro milling process, the tool surface and workpiece pull-off can be considered the separation process between rigid line and substrate. According to Kendall [39], the adhesive contact pull-off stress of a rigid line and substrate can be obtained:

$$\sigma_{pull-off} = \left[\frac{8E\Delta\gamma}{\pi(1-\nu^2R)} \right] \tag{9}$$

where E is Young's modulus and ν is the Poisson ratio. R is the rigid line radius. The end teeth flank of micro end mill contacts aluminum alloy, and aluminum alloy elastic deformation occurs under adhesive stress. Separation force is induced by interfacial adhesion effect $\sigma_{pull-off} \sim R^{-1/2}$. The separation stress increases rapidly with decreasing diameter of tool. Therefore, with diameter reduction of micro end mill, the size

Table 3 Adsorption energy between cemented carbides and aluminum alloy 7075

Adsorption types	Co-Al	Co-Mg	WC-Al	WC-Mg
Adsorption energy (eV)	-7.2455	2.7232	1.8742	3.283

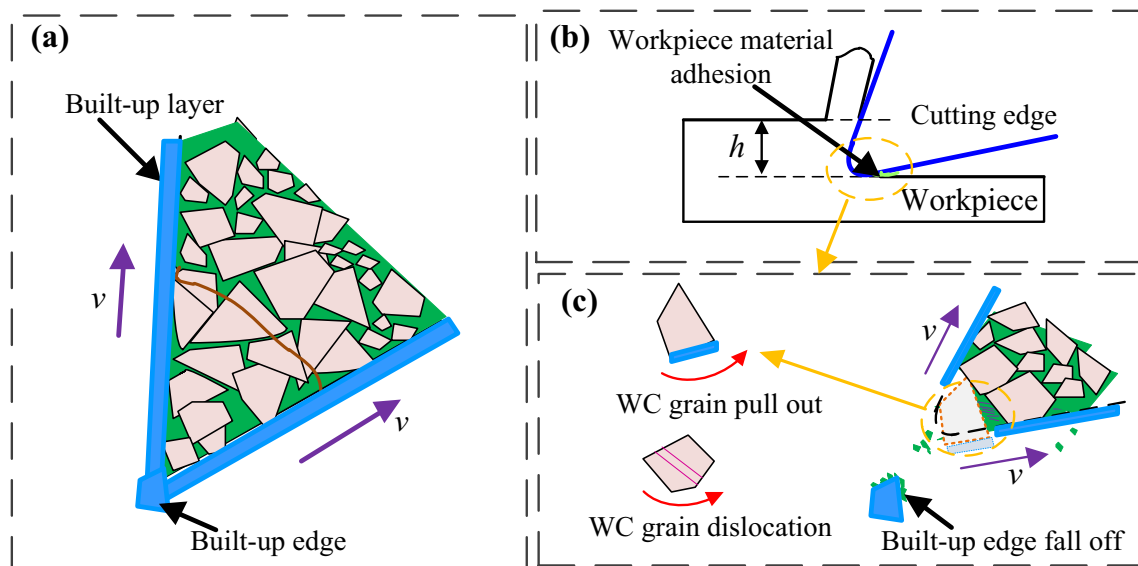


Fig. 12 Adhesive wear damage mechanism of micro end mill

effect of adhesive wear is prevailing and pull-off stress increasing. The tool adhesive wear of micro milling is more serious compared with traditional milling. The micro milling is more prone to adhesive wear compared with traditional milling.

5 Conclusions

The effects of WC grain size and Co content on the microscale wear behavior of cemented carbide micro end mill in aluminum alloy 7075 machining were investigated. The tool wear experiments were performed with different tool materials micro end mills, and the wear morphologies were observed by scanning electron microscope (SEM). The effects of WC grain size and Co content cemented carbides on the tool wear behavior were analyzed. Based on this study, the conclusions are obtained:

- (1) The micro end mill with finer grain size presents better wear resistance. With increase of WC grain size, the end teeth flank wear length of micro end mill increases and the total cutting edge length reduction of the tool obviously increases. Besides, with increase of Co content, the micro end mill exhibits less wear resistance.
- (2) The tool end teeth flank wear length increases with increase of the ratio λ_{Co}/α . In tool material selection of micro end mill, the tool wear resistance can be evaluated by the ratio λ_{Co}/α .
- (3) The damage modes of micro end mills present cutting edge fracture and adhesive wear. Moreover, the built-up edge (BUE) and built-up layer (BUL) occur on the surface of micro end mills. The serious adhesive wear in

cutting edge flank face and the tool tip breakage cause tool failure of micro end mill.

- (4) The adsorption energy between Co atom and Al atom becomes larger based on first principle calculation of adsorption energy between cemented carbides and aluminum alloy. The Co binder of tool material is dragged off by frequent fall off of built-up edge, resulting in more loss of Co element. Thus, the strength of the tool is decreased. Besides, in micro milling, adhesive wear of tool easily occurs and size effect of adhesive wear is prevailing compared with traditional milling.

Funding information This work was supported by National Basic Research Program of China (No. 2015CB059900), National Natural Science Foundation of China (No.51575049) and Basic Research Program (No. DEDPHF).

References

1. Davim JP, Maranh OC, Jackson MJ, Cabral G, Grácio J (2008) FEM analysis in high speed machining of aluminium alloy (Al7075-0) using polycrystalline diamond (PCD) and cemented carbide (K10) cutting tools. *Int J Adv Manuf Technol* 39(11-12): 1093–1100
2. Lei X, Shen B, Sun F (2015) Optimization of diamond coated microdrills in aluminum alloy 7075 machining: a case study. *Diam Relat Mater* 54(1):79–90
3. Li P, Oosterling A, Hoogstrate M, Langen H, Schmidt R (2011) Design of micro square endmills for hard milling applications. *Int J Adv Manuf Technol* 57:859–870
4. Upadhyaya A, Sarathy D, Wagner G (2001) Advances in sintering of hard metals. *Mater Design* 22(6):499–506
5. Llanes L, Torres Y, Anglada M (2002) On the fatigue crack growth behavior of WC–Co cemented carbides: kinetics description, microstructural effects and fatigue sensitivity. *Acta Materialia* 50(9): 2381–2393

6. Guo Z, Xiong J, Yang M, Dong G, Wan W (2012) Tool wear mechanism of WC–5TiC–10Co ultrafine cemented carbide during AISI 1045 carbon steel cutting process. *Int J Refract Met Hard Mater* 35(1):262–269
7. Kai E, Takemoto S, Masao Y (2011) Fabrication and cutting performance of cemented tungsten carbide micro-cutting tools. *Precis Eng* 35:547–553
8. Jawaid A, Che-Haron C, Abdullah A (1999) Tool wear characteristics in turning of titanium alloy Ti-6246. *J Mater Process Technol* 92–93(3):329–334
9. Pirso J, Letunovič S, Viljus M (2004) Friction and wear behaviour of cemented carbides. *Wear* 257(3–4):257–265
10. Saito H, Iwabuchi A, Shimizu T (2006) Effects of Co content and WC grain size on wear of WC cemented carbide. *Wear* 261(2):126–132
11. Chen J, Liu W, Deng X, Wu S (2016) Tool life and wear mechanism of WC–5TiC–0.5VC–8Co cemented carbides inserts when machining HT250 gray cast iron. *Ceram Int* 42(8):10037–10044
12. Kadirgama K, Abou-El-Hossein K, Noor M, Sharma K, Mohammad B (2011) Tool life and wear mechanism when machining hastelloy C-22HS. *Wear* 270(3–4):258–268
13. Oliyai S, Karpas Y (2016) Influence of tool wear on machining forces and tool deflections during micro milling. *Int J Adv Manuf Technol* 84(9–12):1–18
14. List G, Nouari M, Géhin D, Gomez S, Manaud J, Petitcorps Y, Girof F (2005) Wear behaviour of cemented carbide tools in dry machining of aluminium alloy. *Wear* 259(7):1177–1189
15. Wang X, Kwon P (2014) WC/Co tool wear in dry turning of commercially pure aluminium. *J Manuf Sci E-T Asme* 136(3):031006
16. Chen M, Chen N, Guo Y, Wu C, Wang X (2016) Study on the carbide tool wear mechanisms in micro milling stair-shape target of LiF crystal. *Int J Adv Manuf Technol* 84(5–8):1163–1175
17. Konyashin I, Ries B (2014) Wear damage of cemented carbides with different combinations of WC mean grain size and Co content. part II: Laboratory performance tests on rock cutting and drilling. *Int J Refract Met Hard Mater* 45:230–237
18. Konyashin I, Ries B (2014) Wear damage of cemented carbides with different combinations of WC mean grain size and Co content. Part I: ASTM wear tests. *Int J Refract Met Hard Mater* 46:12–19
19. Cantero J, Diaz-Álvarez J, Miguélez M, Marín N (2013) Analysis of tool wear patterns in finishing turning of Inconel 718. *Wear* 297(1–2):885–894
20. Torres Y, Tarrago J, Coureaux D, Tarrés E, Roebuck B, Chan P, James M, Liang B, Tillman M, Viswanadham R, Mingard K, Mestra A, Llanes L (2014) Fracture and fatigue of rock bit cemented carbides: mechanics and mechanisms of crack growth resistance under monotonic and cyclic loading. *Int J Refract Met Hard Mater* 45(45):179–188
21. Sheikh-Ahmad J, Bailey J (1999) The wear characteristics of some cemented tungsten carbides in machining particleboard. *Wear* 225(1):256–266
22. Nouari M, List G, Girof F, Coupard D (2003) Experimental analysis and optimization of tool wear in dry machining of aluminium alloys. *Wear* 255(7):1359–1368
23. Gómez-Parra A, Álvarez-Alcón M, Salguero J, Batista M, Marcos M (2013) Analysis of the evolution of the built-up edge and built-up layer formation mechanisms in the dry turning of aeronautical aluminium alloys. *Wear* 302(1–2):1209–1218
24. Amin A, Ismail A, Khairusshima M (2007) Effectiveness of uncoated WC–Co and PCD inserts in end milling of titanium alloy—Ti-6Al-4 V. *J Mater Proc Tech* 192–193(5):147–158
25. Lee HC, Gurland J (1978) Hardness and deformation of cemented tungsten carbide. *Mat Sci Eng* 33(1):125–133
26. Golovchan VT, Litoshenko NV (2010) The stress–strain behavior of WC-Co hardmetals. *Comp Mater Sci* 49(3):593–597
27. Liu W, Chen ZH, Wang HP, Zhang ZJ, Yao L, Chen D (2016) Small energy multi-impact and static fatigue properties of cemented carbides. *Powder Metall Ment C* 55(5–6):1–7
28. Zhou L, Wang CY, Qin Z (2009) Tool wear characteristics in high-speed milling of graphite using a coated carbide microendmill. *Proc IME B J Eng Manufact* 223(3):267–277
29. Kindermann P, Schlund P, Sockel HG, Herr M, Heinrich W, Görting K, Schleinkofer U (1999) High-temperature fatigue of cemented carbides under cyclic loads. *Int J Refract Met Hard Mater* 17(1–3):55–68
30. Li A, Zhao J, Wang D, Gao X, Tang H (2013) Three-point bending fatigue behavior of WC–Co cemented carbides. *Mater Design* 45: 271–278
31. Liu B, Zhang Y, Ouyang S (2000) Study on the relation between structural parameters and fracture strength of WC-Co cemented carbides. *Mater Chem Phys* 62(1):35–43
32. Torres Y, Anglada M, Llanes L (2001) Fatigue mechanics of WC–Co cemented carbides. *Int J Refract Met Hard Mater* 19(4):341–348
33. Tarragó JM, Roa JJ, Valle V, Marshall JM, Llanes L (2015) Fracture and fatigue behavior of WC–Co and WC–CoNi cemented carbides. *Int J Refract Met Hard Mater* 49:184–191
34. Klünsner T, Marsoner S, Ebner R, Pippan R, Glätzle J, Püschel A (2010) Effect of microstructure on fatigue properties of WC-Co hard metals. *Procedia Eng* 2(1):2001–2010
35. Sánchez JM, Rubio E, Álvarez M, Sebastián MA, Marcos M (2005) Microstructural characterisation of material adhered over cutting tool in the dry machining of aerospace aluminium alloys. *J Mater Process Technol* 164(20):911–918
36. Greenwood JA (1997) Adhesion of elastic spheres. *Proc R Soc Lond A* 453(1961):1277–1297
37. Östberg G, Buss K, Christensen M, Norgren S, Andrén HO, Mari D, Wahnströma G, Reinecke I (2006) Mechanisms of plastic deformation of WC–Co and Ti(C, N)–WC–Co. *Int J Refract Met Hard Mater* 24(1):145–154
38. Östberg G, Farooq MU, Christensen M, Andrén HO, Klement U, Wahnström G (2006) Effect of $\Sigma 2$ grain boundaries on plastic deformation of WC–Co cemented carbides. *Mater Sci Eng A* 416(1–2):119–125
39. Kendall K (2002) The adhesion and surface energy of elastic solids. *J Phys D* 4(8):1186

Publisher's note Springer Nature remains neutral with regard to jurisdictional claims in published maps and institutional affiliations.